

BPC 01144

Computation of optical motion by movement detectors

Werner Reichardt

Max-Planck-Institut für biologische Kybernetik, Tübingen, F.R.G.

Accepted 27 February 1987

Movement detection; Computation; Optical motion

The first part of this paper deals with a system-theoretical approach for the decomposition of multi-input systems into the sum of simpler systems. This approach is applied here to analyse the algorithm which represents the computations underlying the extraction of motion information from the optical environment by biological movement detectors. The second part concentrates on a specific model for motion computation known to be realized by the visual system of insects and of man. These detectors provide the visual system with information on both the velocity and structural properties of a moving pattern. In the third part of this article the properties of two-dimensional arrays of movement detectors are analyzed and their relations to meaningful physiological responses are discussed.

1. Introduction

When I met Manfred Eigen for the first time around 1953, he asked me why I was interested in problems of information processing by the nervous system. I have forgotten the precise answer I gave, but I remember very well that I tried to explain to him my first steps towards a theory of motion computation which was then based entirely on quantitative behavioural experiments by Hassenstein on an insect, the beetle *Chlorophanus viridis*.

The essential elements of this detector theory together with later additions and ramifications have meanwhile been found to be established not only in other species of insects but also in the visual system of man.

Since Manfred has always been interested in the development of ideas at the borderline be-

tween sensory biology and physics, I would like to write this review-like account to keep him informed with the more recent aspects and advances in biological computation of motion information from the optical environment.

This paper does not describe the development of movement-detector theory in chronological sequence. Rather, it begins with more general considerations on the computation underlying the extraction of motion information. From here it proceeds to a specific model of motion computation for which the input-output relation is formulated mathematically both for its time average and as a function of time. Finally, the properties of two-dimensional arrays of movement detectors are analyzed and their relations to meaningful physiological responses are discussed.

2. Decomposition of multi-input systems

The velocity or position of an object or pattern moving in the visual field of an eye is not represented explicitly at the level of the retinal input.

Dedicated to Professor Manfred Eigen on the occasion of his 60th birthday.

Correspondence address: W. Reichardt, Max-Planck-Institut für biologische Kybernetik, Spemannstr. 38, 7400 Tübingen 1, F.R.G.

Each photoreceptor only provides information on the time-dependent local light flux. From this input the nervous system has to compute motion information. How do the signals from the photoreceptors interact in order to obtain this information?

This question relates to the so-called algorithmic level of the problem. An algorithm is considered here as an operation on an input that yields a corresponding output. In formal terms, an algorithm can be thought of as a mapping, or operator, between a space of input signals and a space of output signals. In some cases it is rather easy to devise algorithms for a given computation and to plan corresponding experiments to check whether these algorithms are actually used whereas in other cases, it might be not that easy. For this reason a general approach [1–3] has been developed in the past that represents a classification scheme for simple algorithms or systems. In general, the operators of interest here are nonlinear; the extraction of motion cannot be performed by a linear system [3].

The concept of nonlinearity, however, is much too general. One has to consider a specific class of nonlinear systems. Experiments on the housefly, *Musca domestica*, for instance, have revealed that in the case of an evaluation of motion information the input-output relations are smooth and continuous. There seems to be no 'decision' or discontinuity involved in the fly's motion computations. In other words, the time signals received by the photoreceptors are transformed continuously into the output function, which in the case of the fly might be represented by the flight torque signal generated about the fly's vertical axis. The further considerations, therefore, can be restricted to smooth time-invariant operators with finite memory.

It has been shown [4] that these smooth systems can be represented in a rather straightforward way and this representation allows a canonical classification scheme. Rigorous results [5] ensure that smooth functionals can be approximated by functional polynomials. Mathematical considerations lead to an explicit representation of the output in terms of the input and thereby we are able to compute properties of the output to any

given input function for a large class of systems. In appendix A a few definitions and formulae are derived for n -input systems.

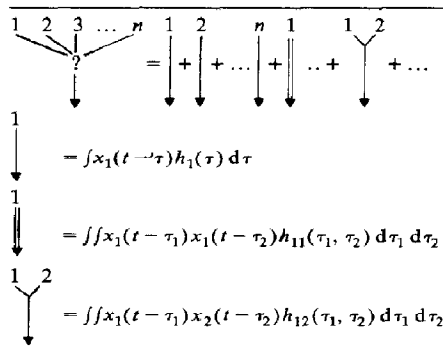
In table 1 a graphical representation of a system is shown, which in our case has many photoreceptors as its inputs. A large class of these systems or their network implementations can be decomposed into an additive sequence of simple canonical systems which are denoted in table 1 by appropriate graphs. In a somewhat similar way, a signal can be decomposed into a series of orthogonal functions of which the Fourier components are only one example. This type of 'language' represents an extension of linear system theory. For instance, linear systems are sufficiently described by the first type of graph in table 1. To each system one may assign a degree (degree 1 for linear systems, degree 2 for bilinear systems, etc.) and a p -order defined as the number of distinct inputs of the system. It is obvious that the p -order is always smaller or equal to the degree of the system.

The important point is that specific properties of information processing can be associated with each of these systems. For instance, 'quadratic' systems can perform computations that linear systems certainly cannot. In particular, in the case of stationary images, it is rather easy to characterize

Table 1

Decomposition of a nonlinear, multi-input system

A large class of multi-input systems can be decomposed into a sum of simpler systems, denoted by appropriate graphs. Each graph is a short-hand notation for an explicit mathematical representation. This power-series development of a system is a generalization of a Taylor series development of a function.



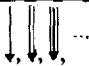


the types of images that can be discriminated by the various graphs.

Besides a classification of the computational properties of a given system, it is also possible to characterize its functional properties. These points will become more evident in the present example of the analysis of algorithms used by the visual system of the fly to compute motion, position and relative motion information. The main theoretical considerations important for motion computation and for the design of critical experiments will be sketched in the following.

3. Directionally selective motion algorithm

If a system is to be defined as directionally selective for motion, it is required that it produces a direction-selective time-averaged response; i.e., motion in a preferred direction must lead to a positive average response, whereas motion in the counter direction must be either ineffective or result in a negative average response. Having defined the computation, one can then classify which graphs in the representation, given in table 1, can implement it, beginning with the simple ones of low degree and p -order. Table 2 shows that the first graphs that can implement the direction of motion are the two-input, degree-2 graphs. In addition, they must at least contain an antisymmetric part.

Table 2

	One-input graphs (systems) are not direction selective. Response $\bar{R}(\phi) \propto \cos \phi$
	A two-input, symmetric graph (system) is not direction selective. $\bar{R}(\phi) \propto \cos \phi$
	A two-input, antisymmetric graph (system) is direction selective and constitutes the simplest graph (system) that can compute directional motion $\bar{R}(\phi) \propto \sin \phi$
Direction selectivity: properties of graphs (systems) for two-input sinusoidal stimulation	

The problem now arises as to how to devise experiments that can tell whether the biological system under investigation, i.e., our model system, the housefly *M. domestica*, is using this simple algorithm or interaction, or whether more complex ones with higher p -order are implemented. Fig. 1 outlines the principle of such an experiment. Movement of a sinusoidally contrasted grating is simulated by flickering two bars sinusoidally with a phase shift ϕ in front of the fly's eye. One may ask for the time-averaged output of each subsystem represented by a graph in table 2 as a function of the phase angle ϕ while the frequency (stripe periods per s) is kept constant. Positive phase is equivalent to motion to the right and negative phase to motion to the left. It is rather easy to show that the average output depends on the phase in a manner that is characteristic for each graph represented in table 2. For instance, one-input systems, irrespective of order, have an output that does not distinguish phases of different sign. However, for second-order, antisymmetric, two-input graphs, the phase dependence of the output is proportional to $\sin \phi$. In general this is not true for higher-order terms. The basic question is, how does a test-fly react under these experimental conditions?

A typical experiment [6] to demonstrate the phase dependence is outlined in fig. 2. The flying test-fly is fixed to a flight-torque compensator (see, e.g., ref. 7), and its torque is measured. Since flies and other organisms tend to follow movement in the environment in order to stabilize their

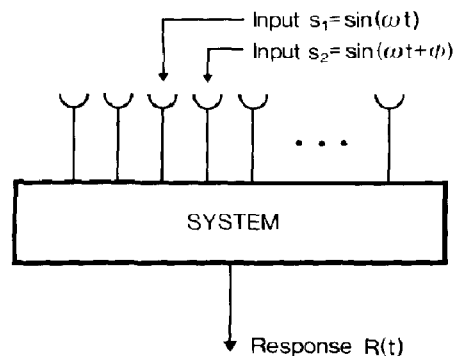


Fig. 1. Sinusoidal stimulation of a pair of photoreceptors.

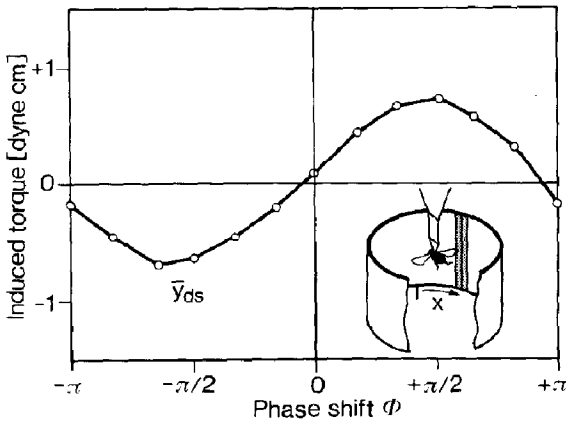


Fig. 2. Mean torque response of a test-fly elicited by two 2.7° -wide vertically oriented filament lamps whose intensities are sinusoidally modulated and phase shifted with respect to one another. The phase lag is defined as positive if the luminance modulation of the right lamp follows that of the left lamp. \bar{y}_{ds} designates the half-difference of the reactions induced by the two lamps and represents the direction-sensitive component of the mean optomotor response (modified from ref. 6).

retinal image, positive torque implies that their movement-detecting system measures movement to the right. Conversely, negative torque implies detection of movement to the left. The experimental results plotted in fig. 2 show that:

(a) When a movement to the right (left) is simulated, the time-averaged response is positive (negative). This observation, of course, excludes subsystems which can be represented by one-input graphs.

(b) The phase dependence, to a good approximation, is proportional to $\sin \phi$.

These findings and many other experimental results imply that the algorithm for directional movement computation can be characterized in terms of two-input, degree-2 graphs.

4. Specific interaction underlying movement computation

Antisymmetric, second-order interactions are a minimal model for movement computation. In other words, they are the interactions of lowest

degree which can compute oriented movement.

Interestingly, second-order interactions are also optimal in terms of the so-called 'resolution limit'. It is well known that the resolving power and acuity of the eye are determined by the angular separation and angular sensitivity distribution of the individual receptors, respectively [8,9]. One can show, in agreement with the Shannon sampling theorem (see eq. A6 in appendix A), that a periodic array of equidistant receptors can resolve uniquely the direction of movement of a periodic grating (wavelength λ) only if $\lambda \geq 2\Delta x$, where Δx denotes the distance between two receptors. The resolution limit $\lambda = 2\Delta x$ is already obtained by second-order interactions between neighbouring receptors. In this case (eq. A6), the time average of the direction sensitive optomotor response is proportional to the so-called geometrical interference term

$$\bar{y}_{ds} \propto \sin \frac{2\pi\Delta x}{\lambda} \quad (1)$$

Nonlinearities of higher order than the second may introduce 'artificial' sampling intervals greater than those physically present in the system: as wide-angle interactions, they can, but need not necessarily, impair rather than improve the resolution limit set by the sampling theorem [10-13].

Second-order interactions are not only 'minimal' and 'optimal'; they also have a number of other characteristic properties [11-13] that can be tested experimentally.

(a) Measurements of the equation describing the interference function (see eq. A6) and its comparison with independent data about the topology of the interactions are consistent with second-order nonlinearities. However, eq. A6 cannot directly distinguish between multiple spacings and nonlinearities of order higher than the second. This difficulty can be circumvented by a two-input stimulation. In this case the experimental data shown in fig. 2 clearly suggest second-order interactions ($N = 2$) for the direction-sensitive component \bar{y}_{ds} .

(b) The mean of the direction-sensitive optomotor response shows the property of 'phase invariance'. One can rather easily show that different temporal Fourier components in the input

functions never interfere in the mean output for interactions up to the second order. As a consequence of this 'superposition property' the mean response does not depend upon the relative phases of the spatial Fourier components of an arbitrary pattern moved at constant speed in front of the photoreceptors. The property of phase invariance, characteristic of second-order interactions, leads to the striking experimental result that two quite different patterns elicit an identical mean optomotor response \bar{y}_{ds} [14,15]. In general, for higher-order nonlinearities phase invariance and superposition do not hold!

(c) A third property can be conjectured on the basis of the essential homogeneity and the restricted spatial range of second-order interactions: the interactions between the different channels should have the same frequency dependence. In other words, the coefficients in eq. A6 should satisfy

$$h_n^*(\omega) = \alpha_n h^*(\omega) \quad \text{for all } n, \quad (2)$$

where the α_n are stimulus dependent factors. This leads to the following property of the mean response

$$\bar{y}_{ds}(\omega, \lambda) = T(\omega) I(\lambda) \quad (3)$$

where the function $T(\omega)$ must approach zero if either $\omega \rightarrow 0$ or $\omega \rightarrow \infty$ [16]. Fig. 3 shows that this is indeed the case: the response depends upon the frequency $\omega/2\pi = w/\lambda$ rather than upon the angular velocity w [8,15,17–20]. Eq. 3 again shows the essential simplicity of the interactive structure underlying movement computation. Psychophysical experiments indicate that in humans the perceived velocity of a horizontally moving stripe pattern depends on both λ and w [21]. Moreover, several other criteria indicating the performance of motion evaluation in humans have been shown to depend, under stationary conditions, on contrast frequency rather than on velocity alone (motion after-effect [22,23]; directionally selective adaptation [24]; contrast sensitivity of moving gratings [25]; contrast threshold of directional selectivity [26,27]). This suggests that movement detection in the fly and in humans is based on essentially the same principle algorithm. One fur-

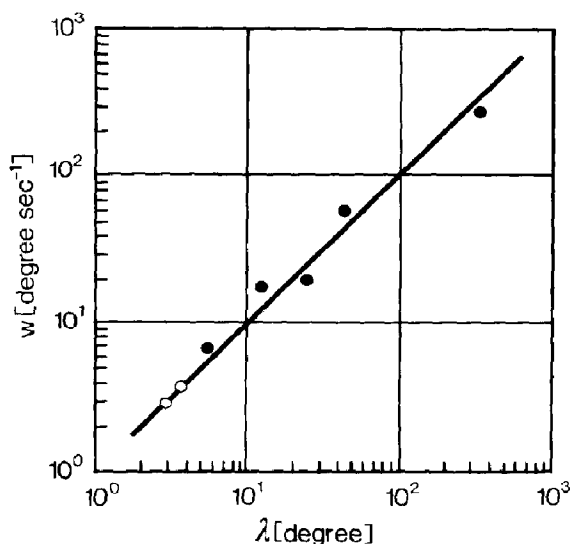


Fig. 3. Relation between wavelength λ of a moving periodic grating and its most efficient velocity w . The maximum reactions, either positive (●) or reversed (○), are determined by the contrast frequency $\omega = w/\lambda$ and not by the pattern velocity w . As a consequence by torque reaction can be factorized into $R(\omega, \lambda) = C(\omega)I(\lambda)$, i.e., ω curves have similar shapes for different λ and vice versa (modified from ref. 19).

ther point is worth mentioning. If a movement detection system does not satisfy eq. 3 this does not necessarily imply the presence of nonlinearities of an order higher than the second: spatial inhomogeneity of the channels' transfer properties may account for any such deviation.

In summary, the direction-sensitive computation is satisfactorily characterized in terms of a regular pattern of second-order interactions between pairs of photoreceptors. In principle, linear terms may be present as well. Although they do not affect the mean output of the movement detector, they may play a significant role with respect to its dynamics.

5. Models of selective motion computation

Psychophysical, behavioural and electrophysiological data have suggested a few specific models of selective motion computation [10,28–40]. Clearly, the formalism discussed before is not a

model of movement computation. Its aim is to illustrate how the design of such a theory may begin, which constraints must be taken into account and which classes of functional models can be experimentally distinguished. One of the first models of movement computation was proposed by Hassenstein and Reichardt [41] and outlined in more detail by Reichardt [28,29] and Hassenstein [42,43]. The scheme, which depends upon evaluating the cross-correlation between signals from two visual elements or neuro-ommatidia, could originally account for the antisymmetric mean optomotor response of the beetle *Chlorophanus*; it has led to predictions which were also experimentally verified in other insects species [9,14,44]. Other versions of the original *Chlorophanus* model were proposed in different contexts [10,45] and, most importantly, with respect to motion perception in man [35–38,40]. They are in fact correlation models, characterized by the time-averaged output

$$\bar{y}_{ds} = \int \tilde{W}(\omega) S_1(\omega) S_2(-\omega) d\omega \quad (4)$$

where $\tilde{W}(\omega)$ is an odd, imaginary function, reflecting the overall filter properties of the network; $S_1(\omega)$ and $S_2(\omega)$ are the Fourier transforms of the time-dependent inputs. It can be shown that the class of correlation models is the most general representation of second-order interactions, if the mean direction-sensitive output is considered. In terms of the classification used before it is also the simplest scheme capable of selective motion evaluation.

The operations of these correlation-type movement detectors have been studied for a long time. Until more recently they have been investigated only under the condition that time averages of their responses were taken. A simplified version of a motion detector of the correlation type and its decomposition into elements responding to motion from left to right and from right to left are shown in fig. 4a–c. The major simplification of the detector made here relates to the low-pass filtering of the input signals which are approximated for convenience by a delay ϵ .

I consider here the case that a one-dimensional contrast pattern $F(x)$ is moved with constant

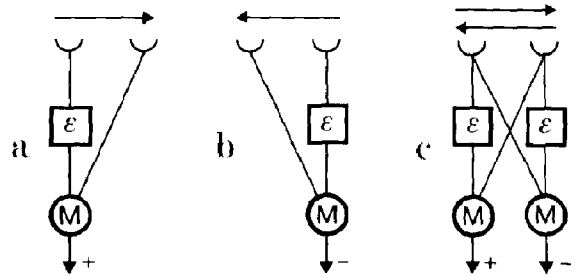


Fig. 4. (a–c) Representation of the operations of movement detectors. Unidirectional (a, b) and bidirectional movement detectors (c) consisting of two light receptors, signal delay ϵ in one or two channels and elementary signal multiplication stages M. As in fig. 3 the preferred direction of movement is shown by the arrows.

velocity w across an individual detector so that $F = F(x \pm wt)$. If the input of the left receptor (see fig. 4c) due to a moving pattern is given by

$$S_1(t) = \sum_{\nu=-\infty}^{+\infty} \frac{a_{\nu}}{2} e^{i\nu\omega t} \quad (5)$$

and that of the right receptor input by

$$S_2(t) = \sum_{\nu=-\infty}^{+\infty} \frac{a_{\nu}}{2} e^{i\nu\omega t} e^{i\nu\phi} \quad (6)$$

where a_{ν} are the coefficients of a Fourier representation of F and ϕ the phase shift between the two input signals and if $H(\omega) = e^{i\epsilon\omega}$ describes the frequency response of the detector filters, simple calculation leads to the time-averaged detector response to motion from left to right

$$\bar{R} = \sum_{\nu=0}^{+\infty} |a_{\nu}|^2 \sin(\nu\omega\epsilon) \cdot \sin(\nu\phi) \quad (7)$$

with $\phi = 2\pi\Delta x/\lambda$ and $\omega = w/\lambda$.

The response \bar{R} of the specific model is proportional to the geometrical interference term $\sin(\nu\phi)$, which corresponds to eq. 1 and, in addition, depends on w/λ , the contrast frequency of the pattern. The superposition property and the property of the phase invariance of Fourier components synthesizing the pattern F which have been mentioned already (item (b) in section 4) are obvious from eq. 7. Most important, however, the structure of eq. 7 is in accordance with eq. 2 which was

originally derived from eq. A6 for second-order interactions.

6. Continuous approach of the second p -order motion-detector model

So far, the time-averaged response of the correlation model for motion computation has been described. Theoretical insights into the dynamics of the detector and its comparison with experiments are, of course, only possible if for arbitrary moving patterns the detector inputs can be related to its output as a function of time [46]. This has been done by means of a 'continuous approach'. The distance between adjacent receptors is thereby assumed to be infinitesimally small. This approximation holds if the highest spatial Fourier component of the moving pattern is large compared with dx , the separation of two adjacent receptors. This condition is usually fulfilled in a natural environment.

Here, it is assumed that a one-dimensionally contrast-modulated pattern $F = F(x)$ is moved in front of a detector array. The individual detectors are oriented in the x -direction and a coordinate x^* is associated with the array. Under these conditions, the following expression holds

$$F = F(x^*) \text{ with } x^* = x + s(t) \quad (8)$$

where F represents the contrast pattern function and $s(t)$ a time-dependent spatial displacement of the pattern. Consequently, $ds(t)/dt$ describes the instantaneous pattern velocity. In appendix B, it is shown that the signal output of a motion detector at position x is given, to a first approximation, by the expression

$$dD(x, t) = -\epsilon \cdot \frac{ds(t)}{dt} \cdot S(x, t) dx \quad (9)$$

with

$$S(x, t) = \left(\frac{\partial F}{\partial x} \right)^2 - F \frac{\partial^2 F}{\partial x^2} \quad (10)$$

In the continuous approach, the output of the elementary detector may be expressed as a response density $dD(x, t)/dx$. Higher approxima-

tions of the response density can be derived from a generalized theory which has been recently established [47]. The generalized theory represents an approximation of n -th order, provided that the pattern $F(x)$ can be developed into a convergent Taylor series. Interestingly, in eq. 9 the pattern velocity appears as a separate factor. The response of the elementary detector is only different from zero if $ds/dt \neq 0$ and $(\partial F/\partial x)^2 \neq F \cdot \partial^2 F/\partial x^2$. The second condition is usually fulfilled. One exception consists of a pattern given by an exponential function $F = F_0 e^{\pm a(x+s(t))}$. Of course, the response of the detector also disappears when the pattern is not contrast modulated, i.e., if $F = F_0 = \text{constant}$. Another interesting case is a pattern of the type $F = A \pm C(x, t)$ with $C = B e^{-a^2(x+s(t))^2}$ which at the level of the detector output leads through eq. 9 to an expression graphically represented in fig. 5 with the parameter settings specified in the figure legend. The result shows that the detectors stimulated by the central part of the particular contrast function signal motion in accordance with the direction of pattern motion whereas the detectors stimulated by the peripheral parts of this function provide signals of apparent counter motion. This predicted property, unknown until recently, has meanwhile been tested in behavioural experiments. In these tests a one-dimensional periodic pattern was moved behind a slit to provide stimulation only to a restricted area of the compound eye of a test-fly. In this way spatial 'integration' can, in principle, be prevented from affecting the time course of the response. A computer simulation of the movement-detector response to motion of a one-dimensional sinusoidal contrast pattern is shown in fig. 6. The sinusoidal pattern is moving from left to right with constant velocity, the response of the detectors being plotted in the lower part of fig. 6. The response to the moving pattern $F(x, t) = A + B \sin k(x - wt)$ is periodic, however, parts of the response profile are negative which means that these detectors signal an inverted response with respect to the direction of motion. From these elementary tests it follows that the instantaneous detector response strongly depends on the structure of the moving pattern which might even lead to signalling of an apparent inversion of the direction of motion. The corre-

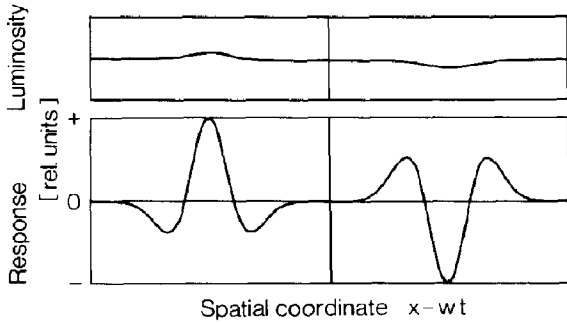


Fig. 5. Response of a linear array of differentially sized movement detectors to a one-dimensional moving contrast pattern. $F(x, t) = A + C(x, t)$ with $C = Be^{-a^2(x-wt)^2}$, where w is the velocity of motion. Parameter settings: $a = 10^{-2}$, $A = 1$, $B = 0.2$. Looking at the detector output channels we observe a signal which moves with the pattern velocity w . The calculated output functions of the movement detectors surprisingly consist of two parts, one which signals the sign of pattern motion in the correct way (+ in the diagram on the left, - on the right), whereas the other part signals apparent counter motion (- in the diagram on the left, + on the right). However, when the integral over all the individual motion contributions is taken, the sign of the integrated detector outputs correctly reflects the actual direction of motion of the pattern.

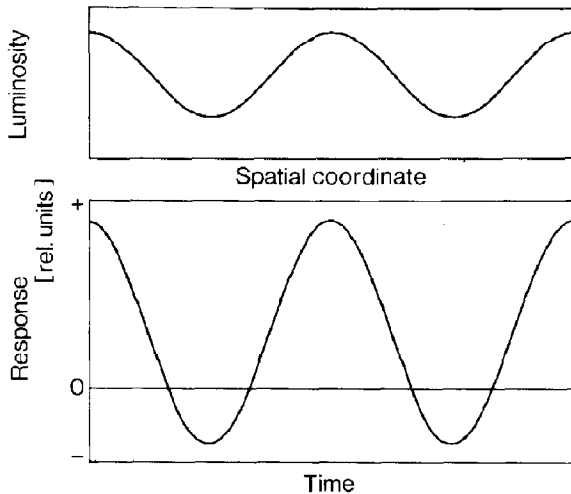


Fig. 6. Response of an array of motion detectors to a moving contrast function. (Upper panel) A one-dimensional contrast $F(x, t) = A + B \sin k(x - wt)$ is moving with constant velocity w from left to right. (Lower panel) Response of a movement detector to the moving contrast function, shown in the upper panel. The response has the same period and phase as the stimulus but partly (its negative parts) signals an apparent counter direction of motion (to the left and not to the right).

sponding experimental result is shown in fig. 7. A sinusoidally contrasted pattern is moved around a test-fly which is fixed in a flight-compensator and the torque response of the fly is measured. The moving pattern is 'seen' by the fly only through a slit. The response recorded in the left part of the diagram corresponds to motion from left to right (R) and in the right part to motion from right to left (L). One can easily see that the periodic response of the torque signals shows a zone of overlap between the two responses to right- and leftwards motion. This result is in accordance with the predicted response and the simulations shown in fig. 6. The time averages in both the computer simulation and the corresponding experiment signal the correct direction of motion.

7. Two-dimensional theory of movement computation through an array of motion detectors

In section 6 it has been shown that second-order motion detectors (or arrays of it) extract both velocity (the term ds/dt in eq. 9) and structural properties of the pattern (the term $S(x, t)$ in eqs. 9 and 10). It is therefore conceivable and has meanwhile been tested experimentally [46] that pattern information enters the visual system through the motion detectors. In order to understand especially the pattern specific properties in detail, one has to develop a two-dimensional theory of movement computation at the level of the motion detectors before one can actually deal with the problem at the level of spatial, physiological integration.

To this end, I am considering here a two-dimensional contrasted pattern $F(x, y)$ that is moving relative to the two-dimensional detector array with a velocity $v_x = ds_x(t)/dt$, $v_y = ds_y(t)/dt$. Under these circumstances, $F = F(x + s_x(t); y + s_y(t))$. For the sake of simplicity, it is assumed here that the detectors of the array are oriented orthogonally, namely, in the x - and y -directions. Quite similarly, as shown in appendix B for one dimension, the velocity vector $\vec{v}(t)$ is, to a first approximation, related to the output vector $v^*(x, y, t)$ by the linear relation

$$\begin{aligned} v_x^* &= c_{11}v_x + c_{12}v_y \\ v_y^* &= c_{21}v_x + c_{22}v_y \end{aligned} \quad (11)$$

which may be written in compact tensorial form like

$$\vec{v} = T^*(x, y, t) \vec{v} \quad (12)$$

where

$$T^* = \begin{bmatrix} c_{11} & c_{12} \\ c_{21} & c_{22} \end{bmatrix}$$

with the elements

$$c_{11} = -\epsilon \left[\left(\frac{\partial F}{\partial x} \right)^2 - F \frac{\partial^2 F}{\partial x^2} \right]$$

$$c_{22} = -\epsilon \left[\left(\frac{\partial F}{\partial y} \right)^2 - F \frac{\partial^2 F}{\partial y^2} \right]$$

$$c_{12} = -\epsilon \left[\frac{\partial F}{\partial x} \cdot \frac{\partial F}{\partial y} - F \frac{\partial^2 F}{\partial x \partial y} \right]$$

$$c_{21} = -\epsilon \left[\frac{\partial F}{\partial y} \cdot \frac{\partial F}{\partial x} - F \frac{\partial^2 F}{\partial y \partial x} \right]$$

depending in a highly nonlinear fashion on the pattern F . Since $c_{12} = c_{21}$, the tensorial relation, eq. 12, is symmetric and consequently T has real eigenvalues and eigenvectors [48].

A good example to demonstrate some of the properties of eq. 12 is a pattern of the type

$$F(x, y) = A + Bf(x)g(y)$$

with

$$f(x) = e^{-a^2 x^2} \quad \text{and} \quad g(y) = e^{-b^2 y^2} \quad (13)$$

For parameter values of, for instance, $b^2 = \frac{1}{3}a^2$, the Gaussian contrast pattern is plotted in fig. 8a. If the pattern is moved with constant velocity in the x -direction, one obtains at a particular instant of time for the two-dimensional array of x -detectors the response profile which is plotted in fig. 8b. As already pointed out in connection with fig. 6, those x -detectors which receive inputs from the periphery of the Gaussian pattern produce negative responses. This means that they signal apparent motion of the pattern which is opposite to the real motion. Fig. 8c contains the responses of the y -detectors to pattern motion in the x -direction. The response shows a typical feature of the tensorial relation according to eq. 12: The y -de-

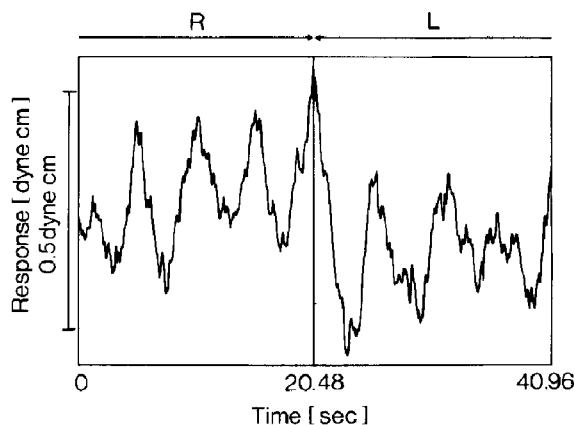


Fig. 7. Optomotor responses of fixed flying test-flies (*M. domestica*), as indicated in fig. 2 to a moving environment. In these experiments the cylindrical environment consisted of a striped pattern with sinusoidal contrast modulation in the horizontal direction which was moved for 20.48 s to the right (R) and for the same time to the left (L). During the motions the velocity was constant and its contrast frequency amounted to $|\omega/\lambda| = 0.19 \text{ s}^{-1}$. The test-flies were exposed to the specific environment where each compound eye was 'looking' through a slit of 8° width which was cut into an opaque white cylinder in order to prevent spatial integration of the visual system as much as possible. The experimental result follows roughly the theoretical prediction shown in fig. 6. Note that the responses to right (R) and left (L) motion partly overlap in strength as a consequence of the periodically changing sign or direction (fig. 6).

tector responses are different from zero in spite of the fact that the pattern is moved orthogonally to the orientation of the y -detectors. A combination of the representations shown in fig. 8b and c is given in fig. 8d in terms of the x - and y -dependent local vectorial responses of pairs of detectors. Again, in spite of the fact that the pattern is moved in the x -direction, most of the local vectorial responses point in different directions, depending on the pattern properties such as local gradients and symmetry. These features become even more apparent when the pattern is rotated by, for instance, 30° (see fig. 9a) but is still moved along the x -direction of the detector array. The local vectorial responses to this pattern are represented in fig. 9b.

In a special class of patterns the off-diagonal

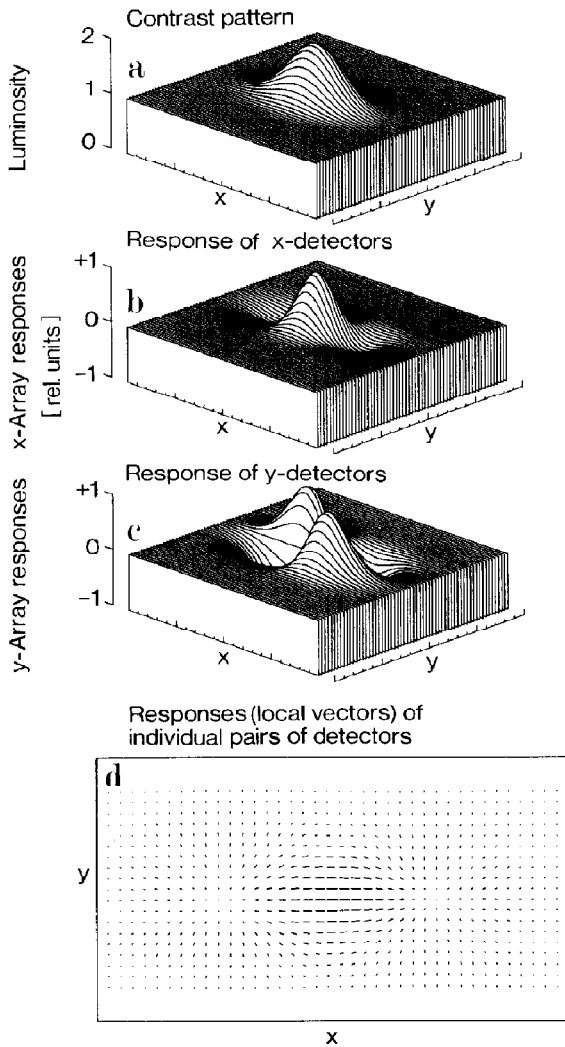


Fig. 8. (a–d) Computer simulation of arrays of orthogonally oriented pairs of elementary motion detectors. The detectors are pointing in either the x - or y -direction. (a) Asymmetric Gaussian contrast pattern whose long axis is pointing in the x -direction. (b) Response of the two-dimensional arrays of x -detectors to motion of the contrast pattern in the x -direction at a particular instant of time. The response profile indicates that those detectors which receive their inputs from the flanks of the pattern respond negatively, i.e., they signal an apparent motion of the pattern in the wrong direction. (c) Responses of the arrays of y -detectors to motion of the contrast pattern in the x -direction. The response profile indicates that the y -detectors respond to motion perpendicular to the orientation of the detectors. (d) Local vectors generated by the contrast pattern in panel a at the outputs of pairs of x - and y -detectors when the pattern is moved in the x -direction. The local vectors point

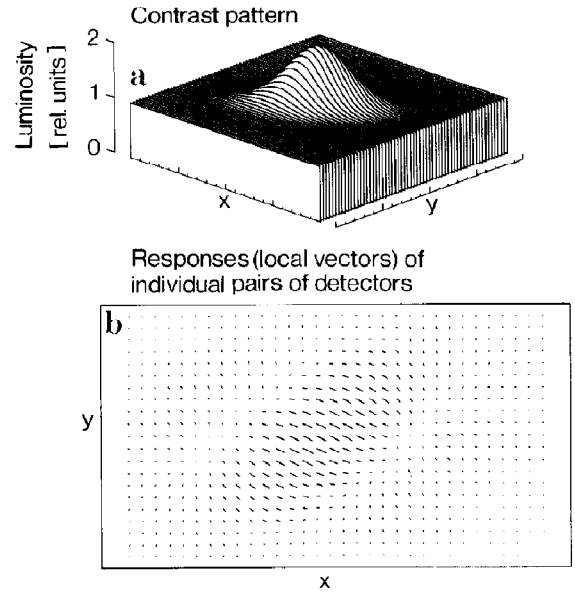


Fig. 9. Computer simulation of arrays of orthogonally oriented pairs of elementary motion detectors. The orientation of the detectors is in the x - and y -directions, respectively. (a) The same contrast pattern as described in fig. 8a, but rotated by 30° . (b) Local vectors at the outputs of individual pairs of x - and y -detectors when the pattern is moved in the x -direction. The local vectors point in different directions. In this case the resulting vectors obtained by integration of the individual responses deviate from the direction of the velocity vector.

elements of the tensor in eq. 12 disappear. This class may, in principle, be found by setting the off-diagonal elements zero which leads to the following differential equation

$$\frac{\partial F}{\partial x} \cdot \frac{\partial F}{\partial y} = F \cdot \frac{\partial^2 F}{\partial x \partial y} \quad (14)$$

A solution of eq. 14 is given by patterns which are separable into purely x - and y -dependent components

$$F(x, y) = f(x)g(y) \quad (15)$$

where the 'background illumination' A in eq. 13 is

in different directions in spite of the fact that the pattern is moved in the x -direction. Mathematical integration in x and y , however, leads in this case to a resulting vector parallel to the velocity vector.

0. For this class of patterns, eq. 12 is reduced to

$$v_x^* = c_{11}v_x \quad \text{and} \quad v_y^* = c_{22}v_y \quad (16)$$

The \vec{v} and \vec{v}^* vectors will usually point in different directions, except if $c_{11} = c_{22}$, a condition which leads to the even more restricted class of patterns such as

$$F(x, y) = e^{(c_0x^2 + c_1x + c_2)} e^{(c_0y^2 + c_1y + c_2)} \quad (17)$$

where c_0 , c_1 and c_2 are arbitrary coefficients. This pattern class generates local detector output vectors $\vec{v}^*(x, y, t)$ that point in the same direction as $\vec{v}(t)$.

Interestingly, patterns according to eq. 17 practically do not exist in reality, since a contrasted environment always contains some background illumination, so that natural patterns may in general be described by the expression

$$F(x, y) = A + F(x, y) \quad (18)$$

with A a constant and $F(x, y)$ a contrast-modulation function. Therefore, an arbitrary pattern generates at the level of the movement detector outputs local vectors which generally point in directions different from that of the velocity vector \vec{v} of the pattern. This implies that in almost all cases it is hardly possible to derive satisfactorily the true direction of motion of a pattern from the activity of local motion detectors.

8. Local versus global features of a two-dimensional array of motion detectors

The experimental results and theoretical considerations of the previous sections have shown that individual motion detectors not only extract velocity but, in addition, also respond to structural information of the pattern moved. A remarkable consequence of these properties is that individual detectors and arrays of individual detectors may signal incorrect information with respect to the velocity of a moving pattern and its direction of motion. The deviations of the local response vectors from the direction of pattern motion may cover the entire angular range. Therefore, it is quite clear that some kind of spatial

integration of the individual detector responses is of fundamental importance to 'organize' these responses in such a way that the representation of movement information allows the detectors to act, and to react, in a meaningful way to a visual environment of objects that are moving relative to the detector array.

It is known that the physiological integrations of the detector responses in the x - and y -directions are of essentially nonlinear nature. In spite of this very fact, it is interesting to inquire – at least from a theoretical point of view – as to how much meaningful information is already gained when the detector outputs are integrated mathematically in space.

To this end, let us assume that a pattern of finite size is moved in front of an infinitely large two-dimensional array of movement detectors whose output signals are integrated in time and space. Under these conditions, the four elements of the tensor in eq. 12 no longer depend on x , y and t . They are globally dependent on the moving pattern. Since, in general, the matrix of the tensor elements is not singular, the velocity vector \vec{v} is related to the global reaction vector \vec{v}_G^* by a one-to-one correspondence. The direction of the global reaction vector is pattern dependent and, apart from special cases, different from that of the pattern velocity vector.

These few considerations already show that linear integration of the output of motion detectors certainly does not solve the problem of creating a strictly meaningful global detector representation of the output of an array. The solution may be based on physiological integration by the so-called Figure-Ground discrimination system which physiologically 'integrates' the detector outputs in two dimensions [4,46,49–52]. Much is known about the integration in the x -direction, but less so about that in the y -direction. The processes involved are highly nonlinear. They explain behaviourally measured and electrophysiologically recorded cellular data and have led to an understanding of two problems: the invariance of the response to different sizes of a moved pattern and the dynamic discrimination of object (figure) and ground without binocular clues.

9. Résumé and outlook

When I talked with Manfred Eigen in the 1950's about motion detection it was not at all clear whether the algorithmic solution for local movement computations would also hold for other insect species. Meanwhile convincing evidence has been acquired. Even more surprising are recent psychophysical findings in man which suggest a system of movement detectors seemingly no different (at the algorithmic level) from the correlation-detection mechanism, discussed here in some detail (e.g., refs. 35–37 and 40).

In the early days when we began to work on the movement-detector problem, I tended to believe that the pattern-sensitive effect on the detector output had no significance for the perception of the visual world. In those days we accepted the 'explanation' that this property (originally only known for the time average of a detector output) reflects an unwanted byproduct of imperfect biological motion detection mechanisms. Meanwhile, an approach to the time-dependent solution of the detector problem has been given [46], and it seems more realistic that motion detectors provide the visual system with both velocity- and pattern-specific information. As a consequence two different sensory properties are handled simultaneously by one and the same detector channel. The significance of this feature and its consequences are far from being fully understood.

Attempts have been made to clarify the movement-detector operations not only at the algorithmic but also at the cellular level. In this connection the work of Riehle and Franceschini [53] should be mentioned. These authors have shown, by recording from a movement-sensitive large-field neuron and by stimulating individual light receptors, that the multiplication scheme of the correlation detector, as derived originally from quantitative behavioural experiments, is implemented by the visual system of insects. The large-field neurons, however, integrate the responses from many motion detectors so that the cellular composition and the type of synaptic interactions responsible for local motion detection remain an unsolved physiological problem.

Future research in the area of motion detection

has to resolve a number of problems, for instance, some topological questions, such as whether pairs, triplets or even higher orders of detector compounds operate together. The main problem, however, after having solved the functional properties of the detector's operations, is the spatial physiological integration of the detector output signals. As has been mentioned before, the Figure-Ground discrimination system of insects is one of the physiological integrators with highly nonlinear properties. It spatially integrates the data collected from many movement detectors and selects coherent signals from those regions of the visual environment which represent objects or patterns moving independently of each other and relative to a patterned ground. After what has been said before, it should be clear that these selections are made by evaluation of time- and space-coherent signals – a very consequence of the properties of the movement detectors as described here. Therefore, an understanding of a complex information-processing problem, such as Figure-Ground discrimination, requires a deep insight into the two-dimensional movement-detector problem.

Appendix A

In this section a few definitions and formulae are given for the specific case of a system with n photoreceptor inputs. The transformation of a moving pattern into the time-dependent receptor output depends on the pattern itself and on the relative motion between pattern and photoreceptors. Only a one-dimensional array of receptors is considered. The results obtained here can be used to interpret experimental data and to characterize the underlying interactions (see ref. 54).

The system is assumed to have an n -th order polynomial representation which is given by the equation

$$y(t) = g_0 + \sum_{i=1}^n g_i^* s_i + \sum_{i,j}^n g_{ij}^{*2} s_i s_j + \dots + \sum_{i_1 \dots i_n}^n g_{i_1 \dots i_n} \dots i_n^* s_{i_1} \dots s_{i_n}$$

with

$$g_i \dots i_e^* s_i \dots s_{il} = \int_{-\infty}^{+\infty} \int_{-\infty}^{+\infty} g_i \dots i_l (\tau_1 \dots l) s_{il} \times (t - \tau_1) \dots s_{il}(t - \tau_l) d\tau_1 \dots d\tau_l \quad (A1)$$

This might be considered as a straightforward generalisation of the well known convolution integral. The input functions $s_i(t)$ are defined as

$$s_i(t) = I_i(t) - I_0, \quad (A2)$$

where I_0 is the light intensity value around which the representation, eq. A1, is valid. Receptor i has the spatial coordinate x_i and an angular sensitivity $\rho = \rho_0(x - x_i)$. The input functions $s_i(t)$ can be obtained from the actual stimulus, a space- and time-dependent light intensity distribution which is determined by the transmission function of the pattern, its motion, the possibly time-dependent illumination and $\rho_i(x)$. General formulae [13] provide, for various stimulus configurations, the coefficients b_{ij} which characterize the Fourier series of $s_i(t)$ in the basic frequency ω^*

$$s_i(t) = \sum_j b_{ij} e^{ij\omega^* t} \quad (A3)$$

i being the unit imaginary number.

Application of eq. A1 to yield the network output is then straightforward. For instance, the average output is given by

$$\begin{aligned} \bar{y} = & g_0 + \sum_i G_i(0) b_{i,0} \\ & + \sum_{i,j} \sum_q G_{ij}(q\omega^*, -q\omega^*) b_{i,q} b_{j,-q} \\ & + \sum_{ijh} \sum_{pq} G_{ijh}(q\omega^*, p\omega^*, (-p-q)\omega^*) b_{i,q} \\ & \cdot b_{j,-p-q} + \dots \end{aligned} \quad (A4)$$

Inspection of the above equation shows that quadratic interactions satisfy the important property of 'superposition in the average'. Fourier components do not interfere in the time-averaged output. We now consider two cases which are needed in the paper.

A1. Sinusoidal grating with spatial wavelength λ moving at constant speed w

The basic frequency, called contrast frequency, is here

$$\omega^* = \frac{2\pi}{\lambda} w \quad (A5)$$

and the average output for motion in one direction in front of equally spaced receptors ($x_i - x_{i-1} = \Delta x$) is for the right eye

$$\begin{aligned} \bar{y} &= \bar{y}_{ds} + \bar{y}_{di}, \quad \bar{y}' = \bar{y}_{ds} - \bar{y}_{di} \\ \bar{y}_{ds} &= \sum_{n=1}^{N^*} h_n^*(\omega) \sin\left[n \frac{2\pi\Delta x}{\lambda}\right] \\ \bar{y}_{di} &= \sum_{n=1}^{N^*} k_n^*(\omega) \cos\left[n \frac{2\pi\Delta x}{\lambda}\right] + k_0^*(\omega) \end{aligned} \quad (A6)$$

where \bar{y}_{ds} and \bar{y}_{di} are the direction-sensitive and direction-insensitive components of the average output. N^* depends both on the degree of nonlinearity of the network and on the maximum distance of interacting receptors. The reduced kernels $h_n^*(\omega)$ and $k_n^*(\omega)$ are derived, for $n \geq 1$, from antisymmetric and symmetric components of the crosskernels G , respectively; the self-kernels generate, together with crosskernels of order greater than unity, the terms $k_0(\omega)$. They depend not only on ω but also on I_0 and on the effective contrast of the pattern (function of actual contrast of ρ_0 and of λ). Interestingly, N^* alone does not characterize the order of the network since it also depends on its topology. The 'interference function' \bar{y}_{ds} is an odd function in $1/\lambda$, while \bar{y}_{di} is even in $1/\lambda$, with period $1/\Delta x$. In \bar{y}_{ds} the first zero crossing, for $1/\lambda$ increasing from zero, occurs for $\lambda \geq 2\Delta x$. Thus, the response has the same sign as the direction of movement if $\lambda \geq 2\Delta x$, quite in agreement with Shannon's sampling theorem. Interestingly, the limit $\lambda = 2\Delta x$ is obtained if only second-order interactions are present [11,12].

A2. Two-input networks with sinusoidal inputs

If

$$\begin{aligned} s_1(t) &= L_1 \sin(\omega t) \\ s_2(t) &= L_1 \sin(\omega t + \phi) \end{aligned} \quad (A7)$$

then

$$\bar{y} = \sum_{n=0}^{\frac{1}{2}N} k_{2n}(\omega) \cos n\phi + \sum_{n=0}^{\frac{1}{2}N} h_{2n}(\omega) \sin n\phi$$

where N represents the maximum even degree of nonlinearity of the network. Again the reduced kernels $h_{2n}(\omega)$ and $k_{2n}(\omega)$ are derived from symmetric and antisymmetric components of the kernels G . Under the condition $k_N(\omega) \neq 0$, the dependence of the average output on ϕ characterizes uniquely N and thus the order of nonlinearity of the system.

Appendix B

If the contrast of a moving pattern changes in only one dimension it may be described by the expression

$$F(x, t) = F[x + s(t)] \quad (\text{B1})$$

where F is the pattern contrast function, x a space coordinate, and $s(t)$ a time-dependent displacement. Accordingly, $ds(t)/dt$ represents the time-dependent pattern velocity. F has the important property

$$\frac{\partial}{\partial x} F[x + s(t)] = \frac{\partial}{\partial s} F[x + s(t)]. \quad (\text{B2})$$

If the two light receptors that are feeding a movement detector are located at x -positions x_1 and x_2 , respectively, the input to receptor 1 is given by $F[x_1 + s(t)]$

and to receptor 2 by

$$F[x_2 + s(t)]. \quad (\text{B3})$$

If $x_2 - x_1 = \Delta x$ is sufficiently small, the $F[x_2 + s(t)]$ function may be approximately derived from the $F[x_1 + s(t)]$ function by adding the first term of a Taylor series developed around x_1 , so that

$$F[x_2 + s(t)] \approx F[x_1 + s(t)] + \left(\frac{\partial F}{\partial x} \right)_{x=x_1} dx, \quad (\text{B4})$$

where dx replaces Δx .

Considering the functional structure of an elementary movement detector we arrive at the filter output of the two channels in fig. 4

$$\int_{-\infty}^t h(t-\eta) F[x_1 + s(\eta)] d\eta$$

and

$$\int_{-\infty}^t h(t-\eta) \left\{ F[x_1 + s(\eta)] + \frac{\partial}{\partial x} F[x_1 + s(\eta)] dx \right\} d\eta \quad (\text{B5})$$

with $h(t)$ the responses of the filters to a Dirac-function $\delta(t)$. The expressions in eq. B5 can be rewritten in a short version: $(h * F)$ and $(h * (F + \partial F/\partial x))$. The detector response is the difference of two products:

$$(h * F) \left(F + \frac{\partial F}{\partial x} dx \right) - \left(h * \left(F + \frac{\partial F}{\partial x} dx \right) \right) F,$$

which finally leads to the expression

$$dD(x, t) = \left\{ (h * F) - \left(h * \frac{\partial F}{\partial x} \right) F \right\} dx \quad (\text{B6})$$

with $dD(x, t)$ the time-dependent detector output at x and $\partial D(x, t)/dx$ the detector response density.

The properties of the filters are approximated here by a small delay ϵ . With this assumption, eq. B6 reads

$$\begin{aligned} dD(x, t) &= \left\{ F[x + s(t-\epsilon)] \cdot \frac{\partial}{\partial x} F[x + s(t)] \right. \\ &\quad \left. - F[x + s(t)] \cdot \frac{\partial}{\partial x} F[x + s(t-\epsilon)] \right\} dx. \end{aligned} \quad (\text{B7})$$

For small ϵ , $F[x + s(t-\epsilon)]$ may be approximated by a Taylor term in ϵ

$$\begin{aligned} F[x + s(t-\epsilon)] &= F[x + s(t)] - \frac{\partial}{\partial s} F[x + s(t)] \cdot \frac{ds(t)}{dt} \cdot \epsilon \\ &= F[x + s(t)] - \frac{\partial}{\partial x} F[x + s(t)] \cdot \frac{ds(t)}{dt} \cdot \epsilon \end{aligned}$$

and correspondingly,

$$\begin{aligned} & \frac{\partial}{\partial x} F[x + s(t - \epsilon)] \\ &= \frac{\partial}{\partial x} \left\{ F[x + s(t)] \right. \\ & \quad \left. - \frac{\partial}{\partial x} F[x + s(t)] \cdot \frac{ds(t)}{dt} \cdot \epsilon \right\}. \end{aligned}$$

For $dD(x, t)$ we finally obtain the expression

$$\begin{aligned} dD(x, t) = & \left\{ \left[F - \frac{\partial F}{\partial x} \cdot \frac{ds(t)}{dt} \cdot \epsilon \right] \cdot \frac{\partial F}{\partial x} \right. \\ & \left. - F \frac{\partial}{\partial x} \left[F - \frac{\partial F}{\partial x} \cdot \frac{ds(t)}{dt} \cdot \epsilon \right] \right\} dx \end{aligned}$$

or

$$\frac{dD(x, t)}{dx} = -\epsilon \frac{ds(t)}{dt} \left\{ \left(\frac{\partial F}{\partial x} \right)^2 - F \frac{\partial^2 F}{\partial x^2} \right\} \quad (\text{B8})$$

Eq. B8 represents the first approximation of the response density of an elementary movement detector at position x when excited with a moving pattern.

Acknowledgments

I am indebted to Professor K.G. Götz and Dr. M. Egelhaaf for suggestions and for critically reading the manuscript. In addition, I would like to thank Dr. Götz for the graphics computer program. I also like to thank Mr. Leo Heimbürger for drawing the figures and Mrs. Inge Geiss for typing different versions of the manuscript.

References

- 1 T. Poggio and W. Reichardt, *Kybernetik* 13 (1973) 223.
- 2 T. Poggio and W. Reichardt, in: *Cold Spring Harbor Symp. Quant. Biol.* 40 (1976) 635.
- 3 T. Poggio and W. Reichardt, *Q. Rev. Biophys.* 9 (1976) 377.
- 4 W. Reichardt and T. Poggio, *Biol. Cybern.* 35 (1979) 81.
- 5 G. Palm and T. Poggio, *Math. Biol.* 4 (1977) 375.
- 6 B. Pick, *Z. Naturforsch.* 29c (1974) 310.
- 7 G. Fermi and W. Reichardt, *Kybernetik* 2 (1963) 15.
- 8 K.G. Götz, *Kybernetik* 2 (1964) 77.
- 9 W. Reichardt, in: *Processing of optical data by organisms and machines*, ed. W. Reichardt (Academic Press, New York, 1969) p. 465.
- 10 J. Thorson, *Kybernetik* 3 (1966) 41.
- 11 T. Poggio and W. Reichardt, *Kybernetik* 12 (1973) 185.
- 12 E. Buchner, Dissertation, Eberhard-Karls Universität, Tübingen, (1974).
- 13 G. Geiger and T. Poggio, *Biol. Cybern.* 17 (1975) 1.
- 14 D. Varjú and W. Reichardt, *Z. Naturforsch.* 22b (1967) 1343.
- 15 K.G. Götz, *Bibl. Ophthalmol.* 82 (1972) 251.
- 16 K.G. Götz, *J. Comp. Physiol.* 99 (1975) 187.
- 17 P. Kunze, *Z. Vgl. Physiol.* 44 (1961) 656.
- 18 G.D. McCann and G.F. MacGinitie, *Proc. R. Soc. Lond.* B163 (1965) 369.
- 19 H. Eckert, *Kybernetik* 14 (1973) 1.
- 20 E. Buchner, in: *Photoreception and vision in invertebrates*, ed. M.A. Ali (Plenum Press, New York, London 1984) p. 561.
- 21 H.C. Diener, E.R. Wist, J. Dichgans and T. Brandt, *Vision Res.* 16 (1976) 169.
- 22 A. Pantle, *Vision Res.* 14 (1974) 1229.
- 23 M.J. Wright and A. Johnston, *Vision Res.* 25 (1985) 1947.
- 24 D.J. Tolhurst, *J. Physiol.* 231 (1973) 385.
- 25 D.H. Kelly, *J. Opt. Soc. Am.* 69 (1979) 1340.
- 26 D.C. Burr and J. Ross, *Vision Res.* 22 (1982) 479.
- 27 S.J. Anderson and D.C. Burr, *Vision Res.* 8 (1985) 1147.
- 28 W. Reichardt, *Z. Naturforsch.* 12b (1957) 448.
- 29 W. Reichardt, in: *Principles of sensory communications*, ed. W.A. Rosenblith (Wiley, New York, 1961) p. 303.
- 30 H.B. Barlow and W.R. Levick, *J. Physiol.* 178 (1965) 477.
- 31 J. Thorson, *Science* 145 (1964) 69.
- 32 D.H. Foster, *Kybernetik* 8 (1971) 69.
- 33 O.-J. Grüsser and U. Grüsser-Cornehls, in: *Handbook of sensory physiology*, vol. VII/3A, ed. R. Jung (Springer-Verlag, Berlin, 1973) p. 333.
- 34 A.J. van Doorn and J.J. Koenderink, *Biol. Cybern.* 21 (1976) 161.
- 35 A.J. van Doorn and J.J. Koenderink, *Exp. Brain Res.* 35 (1982) 179.
- 36 A.J. van Doorn and J.J. Koenderink, *Exp. Brain Res.* 45 (1982) 189.
- 37 J.P.H. van Santen and G. Sperling, *J. Opt. Soc. Am.* A1 (1984) 451.
- 38 J.P.H. van Santen and G. Sperling, *J. Opt. Soc. Am.* A2 (1985) 300.
- 39 E.H. Adelson and J.R. Berg, *J. Opt. Soc. Am.* A2 (1985) 284.
- 40 H.R. Wilson, *Biol. Cybern.* 51 (1985) 213.
- 41 B. Hassenstein and W. Reichardt, *Z. Naturforsch.* 11b (1956) 513.
- 42 B. Hassenstein, *Z. Vergl. Physiol.* 40 (1958) 556.
- 43 B. Hassenstein, *Z. Naturforsch.* 14b (1959) 659.
- 44 W. Reichardt and D. Varjú, *Z. Naturforsch.* 14b (1959) 674.
- 45 K. Kirschfeld, in: *Information processing in the visual system of arthropods*, ed. R. Wehner (Springer-Verlag, Berlin, 1972) p. 61.
- 46 W. Reichardt and A. Guo, *Biol. Cybern.* 53 (1986) 285.
- 47 M. Egelhaaf and W. Reichardt, *Biol. Cybern.* (1987) 1.

- 48 W. Reichardt, in: *Complex systems – Operational approaches in neurobiology, physics and computers*, ed. H. Haken (Springer-Verlag, Berlin, 1985) p. 38.
- 49 W. Reichardt, T. Poggio and K. Hausen, *Biol. Cybern.*, Suppl. 46 (1983) 1.
- 50 M. Egelhaaf, *Biol. Cybern.* 52 (1985) 123.
- 51 M. Egelhaaf, *Biol. Cybern.* 52 (1985) 195.
- 52 M. Egelhaaf, *Biol. Cybern.* 52 (1985) 267.
- 53 A. Riehle and N. Franceschini, *Exp. Brain Res.* 54 (1984) 390.
- 54 W. Reichardt and T. Poggio, in: *Theoretical approaches in neurobiology*, eds. W. Reichardt and T. Poggio (MIT Press, Cambridge, MA, 1981) p. 197.